Close to 100 % Renewable Energy Single Family House in Heating Dominated Climates

Fabian Ochs[1], Alice Tosatto[1], Elisa Venturi[1], Alexander Neumann[2]

1 University of Innsbruck, Innsbruck (Austria)

2 AND Holding, Stralsund (Germany)

Abstract

With the goal to reduce the grid electricity demand of new single-family and terraced houses close to zero, an innovative heat supply system based on renewable energy (i.e., PV), heat pumps (HP) and industrialized building-scale long-term thermal energy storage (TES) is investigated by means of a simulation study. The large tank TES is charged using excess PV in summer and supplies heat in winter. The implementation of a booster HP allows to reduce the TES size. The detailed simulation study of the concept shows that in the climate of Rostock (Germany) with a 14 kW_p PV system and a 10 kWh battery the grid electricity demand for appliances and auxiliaries can be reduced from 28 kWh/(m² a) to 5.5 kWh/(m² a). With the TES with a volume of 48 m³ the grid electricity for DHW and SH can be reduced from 11.5 kWh/(m² a) to 2 kWh/(m² a).

Keywords: nearly zero energy building, efficiency, heat pump, thermal energy storage, photovoltaic, P2H

1. Introduction

In heating dominated climates, such as in central Europe, there is a significant mis-match between PV electricity generation with largest shares in summer and the energy demand for space heating (SH) in winter. Hence, for a 100 % renewable energy (RE) supplied building, seasonal storage is required. Seasonal storage for buildings has been investigated for decades and relies predominantly on thermal energy storage (TES). Most promising are large-scale TES applications on district level (Mahon *et al.*, 2022), typically in sub-urban areas and with the goal of increasing the share of renewables (often solar thermal (ST)) but rarely 100 % renewable. In rural areas, presenting a larger share of single-family houses (SFH), district heating is not feasible. With the goal of phasing out fossil-based energy systems, different concepts have been developed and tested. However, seasonal storage on building level is a real challenge in particular from the economic point of view. The Solar House concept suggests large ST and water tanks as e.g. presented by (Kramer et al., 2014). Building-level seasonal storage with ST has been investigated by (Wills, Cruickshank and Beausoleil-Morrison, 2012), and also experimentally shown (Meister and Beausoleil-Morrison, 2021). Integration of a heat pump (HP) coupled with PV enables to increase the solar fraction (Pinamonti et al., 2021) . Seasonal storage using solar thermal and large water tanks in multi-apartment building was investigated by (Ruesch et al., 2022). This concept is well known in Switzerland since many years (Navarro *et al.*, 2016). However, electricity for appliances (APP) and auxiliaries (AUX) is not considered in this concept. A similar concept was investigated by (Al-Addous, 2006) and a correlation between collector area and required water tank volume was delivered as a result of a simulation study. Electricity was disregarded as in most previous works. On building level, sorption TES for SFH has been developed and tested by (Engel et al., 2017). Seasonal thermal storage for a SFH using aluminium storage was investigated by (Haller et al., 2020).

In this contribution an innovative concept for ‘close to 100% RE’ SFH is investigated, which relies on very efficient building envelope, an air-to-water (A/W) HP, mechanical ventilation heat recovery (MVHR), shower drain water recovery (SDWR), PV, battery, buffer storage, and a long-term TES, which once implemented should be produced in an industrialized way and thus potentially will be available at relative low costs.

10.18086/swc.2025.08.08 Available at http://proceedings.ises.org

2. Method

2.1 System Concept

Fig. 1. shows the reference system concept with A/W HP, buffer storage, fresh-water station (FWS), SDWR, PV and battery.

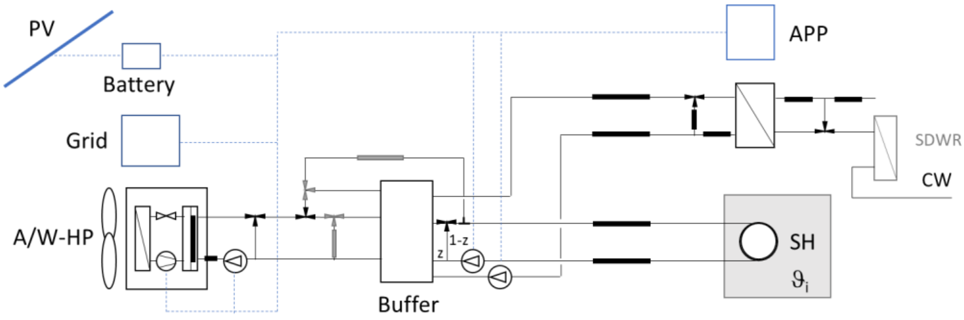

Figure 1: Scheme of the reference system; load (space heating (SH), domestic hot water (DHW) and appliances (APP)); air-to-water (A/W) HP, buffer storage, optional shower drain water recovery (SDWR); PV and battery.

The system concept of the 'close to 100 % RE' system for a SFH is shown in Fig. 2. The booster HP is optional and allows to reduce the volume and/or the temperature level of the long-term TES from 95°C/30°C without to 80°C/10°C. SH is provided by means of a floor heating system at 35°C/30°C and implementing a heating curve (ambient temperature compensation). The HP capacity depends on the building quality, see next sub-section. The size of the PV system, the capacity of the battery and the volume of the TES are varied in a sensitivity analysis.

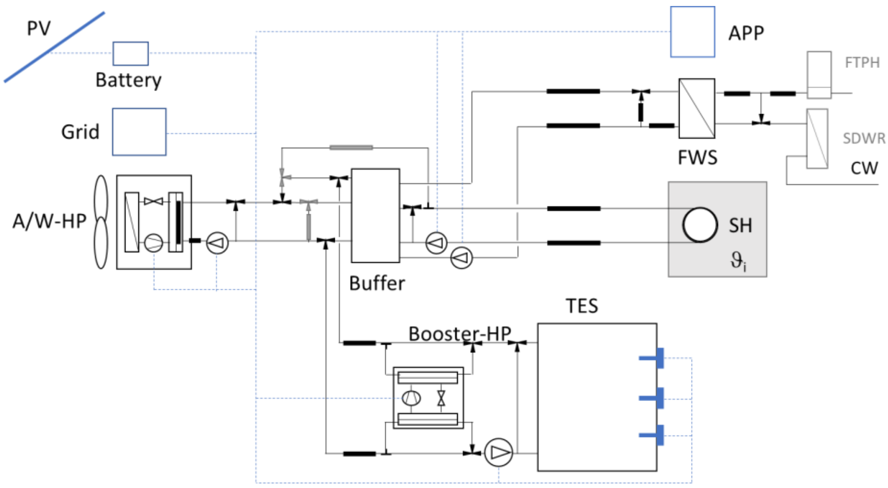

Figure 2: Scheme of the system 'close to 100 % RE' with long-term TES and optional booster HP and optional flow-type post-heater (FTPH).

2.2. Building Variants, Design Parameter

The investigated building is a semi-detached SFH in Rostock, Germany, see Fig. 3.

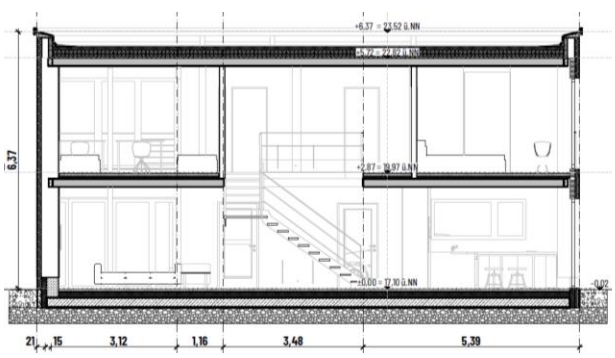

Figure 2: Section of the semi-detached house (Hoppe Architekten), treated area A_T = 144 m².

Different qualities of the thermal envelope are considered ranging from minimum requirements (GEG “Gebäudeenergiegesetz”) to Passive House (PH) quality. Table 1 gives an overview about the investigated building variants and the reference design values of the radiator capacity, HP capacity and buffer volume. Results apply for the climate of Rostock, Germany.

Table 1: Overview of simulated building energy qualities with heating demand (HD), daily average heating load (HL), radiator capacity (C_{RAD}), HP capacity (C_{HP}) and buffer volume (V_{BUF}).

	Building quality				
	“PH”	**“Kfw40+”**	**“Kfw40”**	**“Kfw55”**	**“GEG”**
HD / [kWh/(m² a)]	12.5	17.7	30.5	70.9	82.9
HL / [kWh/(m² d)]	0.21	0.25	0.36	0.64	0.71
C_{RAD} / [kW]	1.3	1.6	2.3	4.0	4.5
C_{HP} / [kW]	1.6	1.8	2.5	4.3	4.7
V_{BUF} / [m³]	0.33	0.34	0.38	0.47	0.49

Domestic hot water (DHW) demand is simulated using DHW profile “M” according to EN 16147. The following design parameters are varied: PV area (A_{PV}), battery capacity (C_{Bat}), buffer volume (V_{buf}), TES volume (V_{TES}), SDWR effectiveness (η_{SDWR}) and power of an optional post-heater (P_{FTPH}).

2.3. Simulation Models

The building is modeled as a lumped mass one-zone model with a simplified one node low temperature heating system. The buffer and the TES are modeled as finite difference models with each 10 nodes. The fresh water HX is based in the ε-NTU approach with each one capacity on the primary and secondary side. It is bypassed on the primary side in times without tapping. A cold-water mixer avoids over-temperature on the secondary side. The EN 16147 tapping profile “M” is applied and energy on the secondary side is only counted if the required useful temperature is achieved, which requires simulation time steps in the range of one to few seconds. Useful energy is counted only when the tapping temperature reaches 45 °C. The SDWR is considered in a simplified way, applying a constant temperature effectiveness of 0.6 for the 2 showers per day. The air/water-(A/W) HP is modeled using the Carnot performance factor approach with a performance factor of η_C= 0.4.

There is one capacity considered at the condenser of the HP. In addition, each pipe of the system is modeled with one node. The battery is modeled using a state-of charge (SoC) approach with one capacity. Auxiliaries for fans, pumps and control are considered. The simulation models are developed in Matlab and the resulting system of ODEs (38 without post-processing) is solved using the ODE23 solver in combination with variable time step with the so-called event detection (based on tapping events and SH control). The electricity balance is solved on simulation time step. PV is first used directly for appliances and auxiliaries. In case of excess PV, the available electric energy is first used to charge the battery and then to run the HP to charge the buffer. If the battery and the buffer are fully charged, excess PV is used to charge the TES. The remaining excess PV is exported to the grid and the remaining energy demand is covered by the grid. Results are post-processed in 300 s time step.

2.4. Key Performance Indicators

The main KPIs are the seasonal performance of the HP(s) and the system (eqs. 1 and 2), the grid energy demand ($w_{el,buy}$), the peak load (PL), the load cover factor (LCF) and supply cover factor (SCF), as presented in eqs. 3 and 4. Furthermore, the TES efficiency is analyzed (eq. 5).

$$SPF_{HP} = \frac{Q_{HP}}{W_{HP}} \quad \text{(eq. 1)}$$

$$SPF_{sys} = \frac{Q_{SH}+Q_{DHW}}{W_{HP}+W_{Pump,HP}+W_{Pump,DHW}+W_{ctr}} \quad \text{(eq. 2)}$$

$$LCF = W_{PV,self}/W_{tot} \quad \text{(eq. 3)}$$

$$SCF = W_{PV,self}/W_{PV,tot} \quad \text{(eq. 4)}$$

$$\eta_{TES} = \frac{Q_{out}}{Q_{in}} \quad \text{(eq. 5)}$$

It is noteworthy that a very efficient TES envelope was assumed with overall heat transfer coefficient of 0.08 W/(m²·K) at top and wall and 0.1 W/(m²·K) at the bottom. This corresponds to an insulation thickness of PUR (λ = 0.032 W/(m·K)) of ca. 40 cm. The TES volume given in the figs. above refers to the water volume.

3. Results

3.1 Influence of climate, building quality and PV size

The influence of the climate, building quality and PV size is investigated prior to the detailed simulations in order to show possible improvements and limits. Simulation results apply for the reference system and are post-processed for different time steps, i.e. hourly, daily, monthly and annually. In addition to the climate of Rostock, the German reference climate (i.e. Potsdam) as well as the Austrian reference climate and the climate of Innsbruck are simulated. Tab. 2 summarizes the monthly global horizontal radiation for the four climates.

Table 2: Monthly global horizontal solar radiation in kWh/(m² month) of the four investigated climates R: Rostock, P: Potsdam, RK Reference climate, IBK: Innsbruck (OIB: Austrian Institute of Construction Engineering)

	1	2	3	4	5	6	7	8	9	10	11	12
R	14	26.8	82.3	129.2	140.8	177.5	164.5	142.1	83.7	57.6	21.5	8.6
P	21.5	29.7	72.2	136.5	164.7	174.3	156.4	134.1	91.9	57.4	22.1	12.6
OIB-RK	29.7	51.6	83.7	112.8	152.3	154.5	159.5	137.8	98	64.2	31.6	22.4
OIB-IBK	32.3	52.9	86.6	113.6	147.4	143.6	151.6	136.1	101.8	66.3	35.9	24.6

As can be seen in Fig. 4 from the annual balance (8760 h), in all cases PV is sufficient to cover the load (LCF = 1) and there is a relevant amount of excess PV (SCF between 55 % and 68 %). With daily storage (24 h), the LCF can be increased from 35 % to 65 % up to 80 % depending on climate building quality and PV size. With monthly storage (672 h) there is a further increase of up to 88 %. Here, the influence of climate, PV size and building quality is strong. With building quality GEG and kfw50, the LCF reaches only 70 % compared to 80 %, with monthly storage. Therefore, further investigation will be conducted only for the higher building qualities (i.e. kfw40, kfw40plus, PH).

The minimum grid electricity demand ($w_{el,buy}$) depends on the PV size, the capacity of the battery and the climate. For Rostock with a 12 kW_p PV system and a 12 kWh battery it is ca. 5.5 kWh/(m² a) and 5 kWh/(m²·a) with a 14 kW_p PV system with 14 kWh battery. Further increasing PV and battery capacity would only lead to marginal improvements. The limit is the very low available solar radiation in winter. Instead, for the climate of Innsbruck (OIB-IBK) because of relevantly more solar radiation in winter the $w_{el,buy}$ is 1.5 kWh/(m²·a) for 14 kW_p and 14 kWh and further increasing PV area and battery size would further reduce it. In the following a battery with a capacity of 10 kWh is assumed.

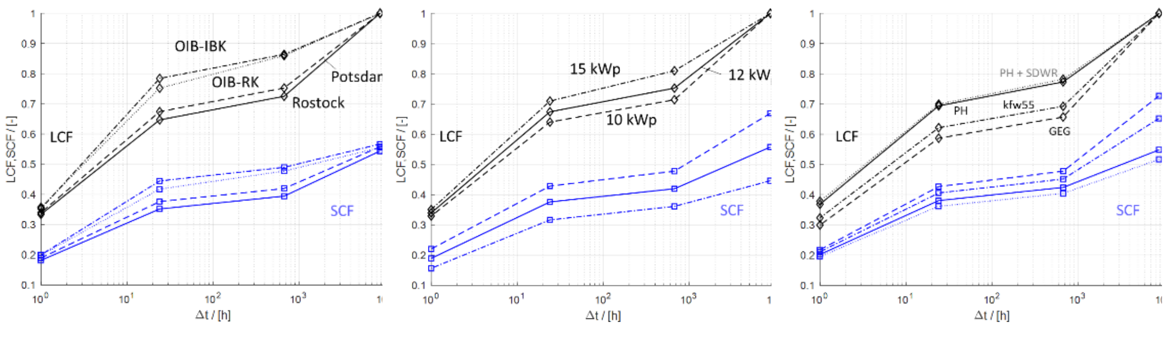

(a) climate (kfw55, 12 kW_p) (b) PV field size (kfw55, Rostock) (c) Building quality (10 kW_p, Rostock)

Figure 4: LCF and SCF as a function of the storage duration from hourly (1 h), to daily (24), monthly (672) and ideal seasonal (8760 h), i.e. net balance.

3.2 Electric Energy Balance

Reference system

The lower limit of the grid electricity demand is 5.8 kWh/(m²·a) (for APP and AUX) for the climate of Rostock and with a PV field size of 12 kW_p and a battery capacity of 10 kWh. Including the SH and DHW, in the reference system the grid electricity demand increases depending on the quality of the building to 15.5 kWh/(m²·a) (for PH) to 21 kWh/(m²·a) (for kfw40+). Even if the PV field size is increased to 20 kW_p, the grid electricity demand remains at 13 kWh/(m²·a), see Fig. 5.

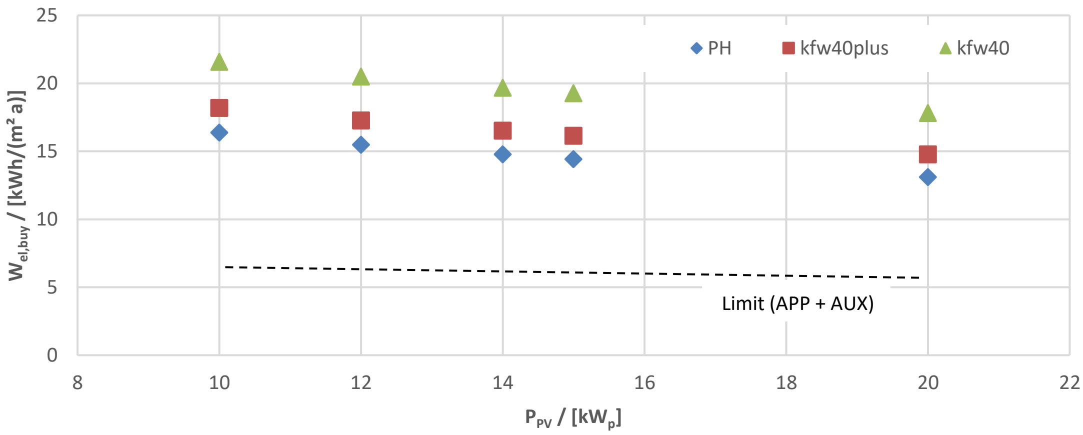

Figure 5: Grid electricity demand for the reference case (w/o TES) for different building qualities and PV sizes (10 kWh battery, Rostock).

Seasonal TES - Influence of Building Quality and Storage Volume

The lower limit of required grid electricity is again indicated by the dashed line in Fig. 6, here 5.8 kWh/(m²·a) for APP and AUX. In case of a very efficient building (PH quality), with 14 kW_p of PV and a TES volume of 48 m³ the total electricity demand can be reduced down to 7.5 kWh/(m²·a). Further increase of the TES volume has only minor influence in this case. For the same volume of the TES, the grid electricity demand is 9.3 kWh/(m²·a) in case of lower building quality (kfw40+). A TES volume of 66.2 m³ and a 14 kW_p PV field would be required to achieve similar grid electricity demand as for the PH quality.

In conclusion, prerequisite for achieving a 'close to 100 % RE' SFH is a very efficient building with PH-quality components and MVHR as well as with SDWR. The grid electricity can be significantly reduced with increasing PV field size (10 kW_p, 12 kW_p, 14 kW_p) and increasing TES volume.

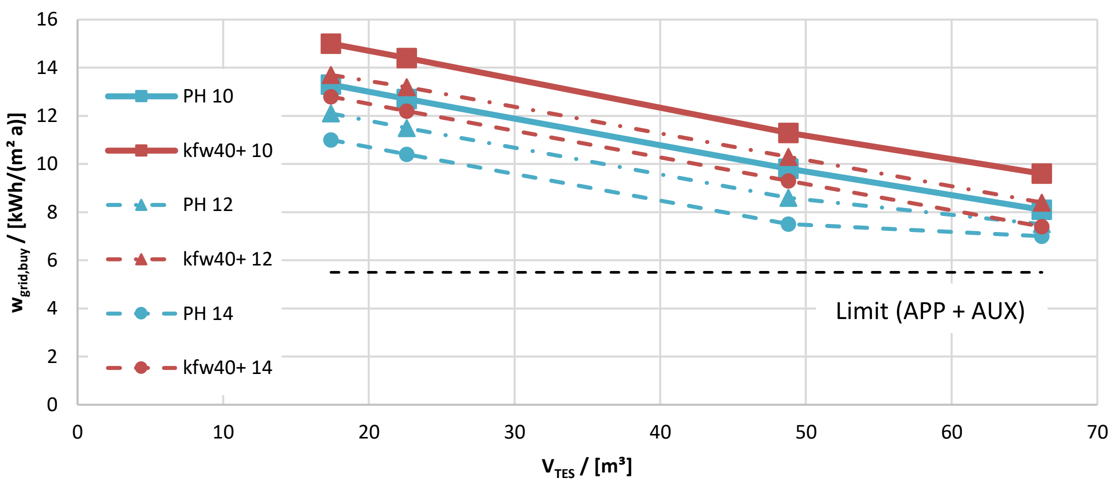

Figure 6: Specific grid electricity demand vs. TES volume for different building energy qualities (PH, kfw40+, kfw40) and PV field sizes (10 kW_p, 12 kW_p, 14 kW_p), without booster HP (Rostock).

3.3 Detailed Analysis

For the example of PH with 12 kW_p, 10 kWh and a TES volume of 48.8 m³, daily average of electric energies (W) are shown together with the state of charge of the battery as well as the buffer and TES temperatures. A summary of the annual integrated energies is given in Tab. 3.

Table 3: Overview of annual thermal (Q) and electric energies (W) .

Thermal		Electric	
Q_{SH} / [kWh/(m² a)]	1780	$W_{el,APP}$ / [kWh/(m² a)]	3886
Q_{DHW} / [kWh/(m² a)]	1520	$W_{el,AUX}$ / [kWh/(m² a)]	713
Q_{HP} / [kWh/(m² a)]	1476	$W_{el,HP}$ / [kWh/(m² a)]	584
$Q_{buf,ch}$ / [kWh/(m² a)]	4283	$W_{el,PV}$ / [kWh/(m² a)]	12343
$Q_{buf,dis}$ / [kWh/(m² a)]	3903	$W_{el,PV,self}$ / [kWh/(m² a)]	9791
$Q_{tes,ch}$ / [kWh/(m² a)]	5754	$W_{el,tes,ch}$ / [kWh/(m² a)]	5754
$Q_{tes,dis}$ / [kWh/(m² a)]	2796	$W_{el,grid}$ / [kWh/(m² a)]	1220

The SPF of the HP is SPF_{HP} = 2.62, the efficiency of the TES (eq. 5) is 0.49. The battery has an efficiency of 90 %. From the results presented in Fig. 7, the following can be observed: PV contribution is negligible in December and January; the battery SoC is at minimum most of the time between November and February (center left); APP and AUX have to be predominantly supplied by the grid in this period. In early spring PV is already used to charge the TES. It is fully charged around July, from then on TES charging only compensates the TES losses. TES discharge starts mid-October. The buffer set-point is increased in winter time when it is charged by the TES to increase the effective buffer volume (top right). In summer, when charged by the HP, the buffer set point temperature is reduced to guarantee efficient operation of the HP. There is a relevant PV excess from July to September (top left).

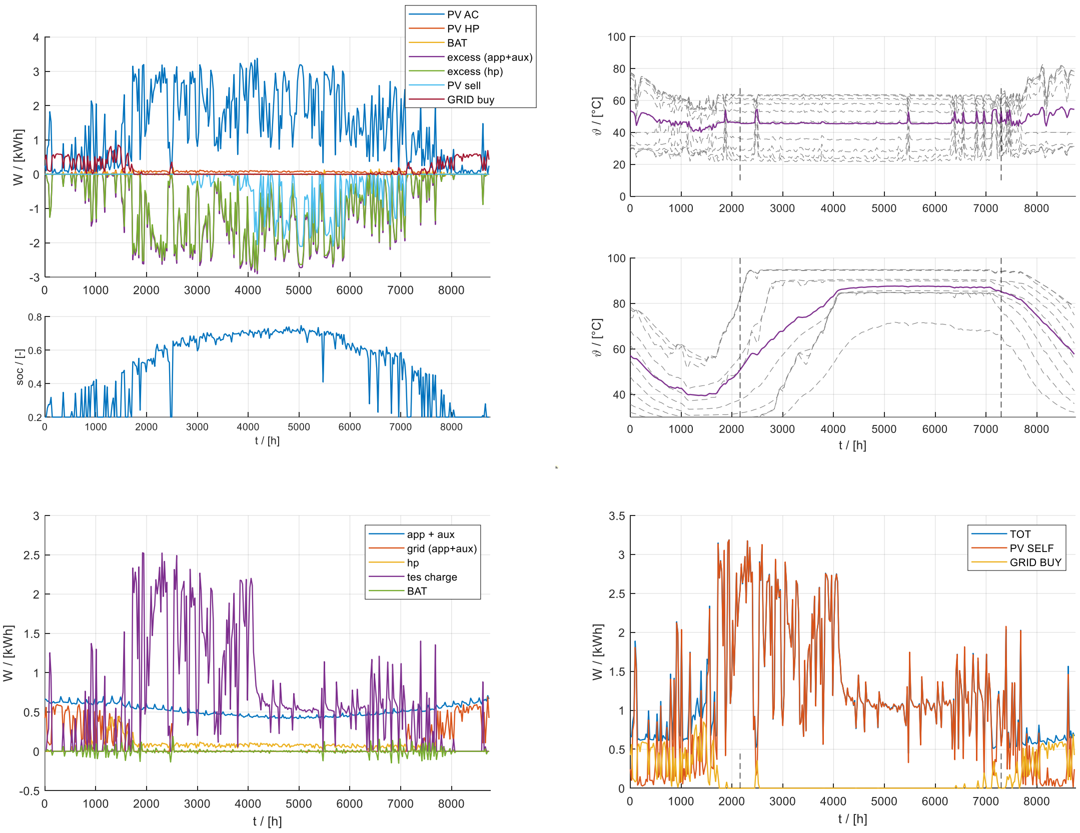

Fig. 7. Daily sum of the energy flows over the course of the year without booster: (top left) PV electric energy balance, (center left) state of charge of the battery, (bottom left) electricity demand (top right) temperatures of the buffer (center right) temperatures of the TES (bottom right) PV-Grid balance, total, self-consumption and remaining grid electricity.

3.4 Booster HP and TES efficiency

With the booster HP, for achieving the same grid electricity demand, either the temperature level of the TES can be reduced (e.g., from 95 °C to 80 °C), which allows for more cost-effective materials and construction of the TES, or with the same temperature level, the volume of the TES can be reduced. The TES efficiency is, because of the high temperature of 95 °C and the long storage period, at only 50%. Due to the decrease of the temperature 80 °C, using the booster HP an increased TES storage efficiency of 62 % can be achieved. The booster HP is in operation from end of December until end of February (with some negligible contributions in March), see Fig. 8.

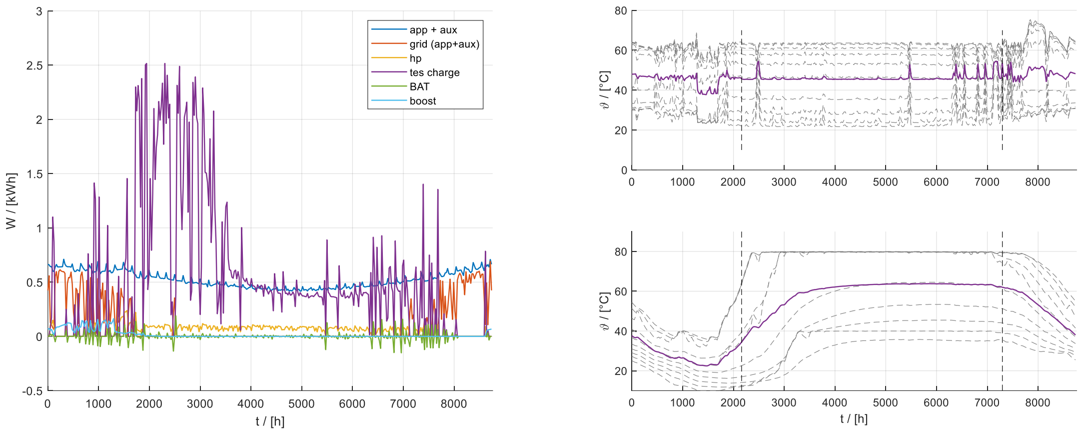

Fig. 8. Daily sum of the energy flows over the course of the year for the case with booster HP: (left) electricity demand (top right) temperatures of the buffer (bottom right) temperatures of the TES; PH, 12 kW$_p$, 10 kWh and 48.8 m³

Tab. 4 summarizes the annual thermal and electric energies for the example of PH with 12 kW$_p$, 10 kWh and a TES volume of 48.8 m³. The SPF of the booster HP is 4.8. The electricity for the booster needs to be bought from the grid, hence grid electricity increases slightly from 1220 kWh to 1288 kWh and the PV self-consumption reduces from 9791 kWh to 8718 kWh.

Table 4: Overview of annual thermal (Q) and electric energies (W).

Thermal		Electric	
Q_{HP} / [kWh/(m² a)]	1363	$W_{el,HP}$ / [kWh/(m² a)]	520
Q_{boost} / [kWh/(m² a)]	721	W_{boost} / [kWh/(m² a)]	150
$Q_{buf,ch}$ / [kWh/(m² a)]	4256	$W_{el,PV}$ / [kWh/(m² a)]	12343
$Q_{buf,dis}$ / [kWh/(m² a)]	3887	$W_{el,PV,self}$ / [kWh/(m² a)]	8718
$Q_{tes,ch}$ / [kWh/(m² a)]	4654	$W_{el,tes,ch}$ / [kWh/(m² a)]	4654
$Q_{tes,dis}$ / [kWh/(m² a)]	2789	$W_{el,grid}$ / [kWh/(m² a)]	1288

4. Conclusions and Outlook

This contribution investigates, based on an extensive simulation study, possibilities and limits of reaching close to autarkic operation of SFH in rural areas in northern Germany. The results demonstrate that full energy autarky cannot be achieved for the analyzed system. The grid electricity demand for the HP for SH and DHW can be reduced to nearly zero by means of a large TES, but electricity for APP and AUX under the climatic conditions of Rostock, Germany remains at ca. 6 kWh/(m² a). Even with optimized system configurations, external energy exchange with the grid remains necessary, especially during winter months with low solar availability. To approach near-autarky, a very high building energy efficiency standard is prerequisite. Building efficiency at the level of Passive House or KfW40+ are minimum requirements, while configurations corresponding to KfW40 show limited feasibility and KfW55 or GEG-compliant designs clearly fail to meet the target.

On the electrical side, PV expansion beyond 10 kW$_p$ provides only moderate improvements; increasing the array size to 12 or 14 kW_p reduces grid import marginally. Similarly, increasing battery capacity from 10 kWh to 12 kWh does not lead to relevant improvements proving that short-term storage has only a limited effect in terms of autarky level. Long term TES plays a crucial role. However, storage volumes of at least 35 m³ with excellent insulation are required to balance seasonal mismatches between generation and demand. A booster HP can offer advantages in terms of storage volume reduction, more relevantly for KfW40+/KfW40 than for PH standard.

Overall, near-autarkic operation with onsite PV and battery capacities is only feasible through an integrated approach combining highest building efficiency and well-insulated long-term storage. However, the grid remains indispensable to ensure reliability during winter. Future work should focus on optimizing the interaction with renewable electricity grids in particular wind power-to-heat to support flexibility and avoid curtailment and to enhance system integration and resilience.

5. Acknowledgments

This contribution was possible through the support of AND Holding UG.

6. References

Al-Addous, M. (2006) *Berechnen der Größe von Wasserspeichern zum saisonalen Speichern von Wärme bei der ausschließlichen Wärmeversorgung von Häusern mit Solarkollektoren*.

Engel, G. *et al.* (2017) 'Simulation of a seasonal, solar-driven sorption storage heating system', *Journal of Energy Storage*, 13, pp. 40–47. Available at: https://doi.org/10.1016/j.est.2017.06.001.

Haller, M.Y. *et al.* (2020) 'Seasonal energy storage in aluminium for 100 percent solar heat and electricity supply', *Energy Conversion and Management: X*, 5. Available at: https://doi.org/10.1016/j.ecmx.2019.100017.

Kramer, W. *et al.* (2014) 'Solar-active-houses - Analysis of the building concept based on detailed measurements', in *Energy Procedia*. Elsevier Ltd, pp. 895–903. Available at: https://doi.org/10.1016/j.egypro.2014.02.103.

Mahon, H. *et al.* (2022) 'A review of thermal energy storage technologies for seasonal loops', *Energy*. Elsevier Ltd. Available at: https://doi.org/10.1016/j.energy.2021.122207.

Meister, C. and Beausoleil-Morrison, I. (2021) 'Experimental and modelled performance of a building-scale solar thermal system with seasonal storage water tank', *Solar Energy*, 222, pp. 145–159. Available at: https://doi.org/10.1016/j.solener.2021.05.025.

Navarro, L. *et al.* (2016) 'Thermal energy storage in building integrated thermal systems: A review. Part 1. active storage systems', *Renewable Energy*. Elsevier Ltd, pp. 526–547. Available at: https://doi.org/10.1016/j.renene.2015.11.040.

Pinamonti, M. *et al.* (2021) 'Water-to-water heat pump integration in a solar seasonal storage system for space heating and domestic hot water production of a single-family house in a cold climate', *Solar Energy*, 213, pp. 300–311. Available at: https://doi.org/10.1016/j.solener.2020.11.052.

Ruesch, F. *et al.* (2022) *SensOpt – Sensible saisonale Wärmespeicherung optimal eingesetzt für die vollständig solare Beheizung von Mehrfamilienhäusern*. Rapperswil. Available at: www.bfe.admin.chwww.hslu.ch/tes.

Wills, A., Cruickshank, C.A. and Beausoleil-Morrison, I. (2012) 'Application of the ESP-r / TRNSYS co-simulator to study solar heating with a single-house scale seasonal storage', in *Energy Procedia*. Elsevier Ltd, pp. 715–722. Available at: https://doi.org/10.1016/j.egypro.2012.11.081.